Cellular and Molecular Neurobiology (2019) 39:241–254
https://doi.org/10.1007/s10571-018-0644-z

ORIGINAL RESEARCH

Retinoic Acid-Induced Protein 14 (RAI14) Promotes mTOR-Mediated Inflammation Under Inflammatory Stress and Chemical Hypoxia in a U87 Glioblastoma Cell Line

XiaoGang Shen[1,2] · JiaRui Zhang[1,2] · XiaoLong Zhang[1,2] · YiFan Wang[1,2] · YunFeng Hu[1,2] · Jun Guo[1,2,3]

Received: 25 August 2018 / Accepted: 8 December 2018 / Published online: 15 December 2018

Abstract

Retinoic acid-induced 14 is a developmentally regulated gene induced by retinoic acid and is closely associated with NIK/NF-κB signaling. In the present study, we examined the effect of RAI14 on mTOR-mediated glial inflammation in response to inflammatory factors and chemical ischemia. A U87 cell model of LPS- and TNF-α-induced inflammation was used to investigate the role of RAI14 in glial inflammation. U87 cells were treated with siR-RAI14 or everolimus to detect the correlation between mTOR, RAI14, and NF-κB. $CoCl_2$-stimulated U87 cells were used to analyze the effect of RAI14 on mTOR-mediated NF-κB inflammatory signaling under chemical hypoxia. LPS and TNF-α stimulation resulted in the upregulation of RAI14 mRNA and protein levels in a dose- and time-dependent manner. RAI14 knockdown significantly attenuated the level of pro-inflammatory cytokine via inhibiting the IKK/NF-κB pathway. Treatment with an mTOR inhibitor (everolimus) ameliorated NF-κB activity and IKKα/β phosphorylation via RAI14 signaling. Notably, RAI14 also enhanced mTOR-mediated NF-κB activation under conditions of chemical hypoxia. These findings provide significant insight into the role of RAI14 in mTOR-induced glial inflammation, which is closely associated with infection and ischemia stimuli. Thus, RAI14 may be a potential drug target for the treatment of inflammatory diseases.

Keywords RAI14 · Neuroinflmamation · mTOR · NF-κB · Chemical hypoxia

Abbreviations

4EBP1	Eukaryotic initiation factor 4E binding protein1
CNS	Central nervous system
$CoCl_2$	Cobalt chloride
Co-IP	Co-immunoprecipitation
eIF4E	Eukaryotic translational initiation factor 4 epsilon
Evero	Everolimus

XiaoGang Shen and JiaRui Zhang have contributed equally to this work.

Electronic supplementary material The online version of this article (https://doi.org/10.1007/s10571-018-0644-z) contains supplementary material, which is available to authorized users.

✉ Jun Guo
guoj@njucm.edu.cn

XiaoGang Shen
20161041@njucm.edu.cn

JiaRui Zhang
184344160@qq.com

XiaoLong Zhang
326310506@qq.com

YiFan Wang
404872122@qq.com

YunFeng Hu
1518498082@qq.com

[1] State Key Laboratory Cultivation Base For TCM Quality and Efficacy, School of Medicine and Life Science, Nanjing University of Chinese Medicine, Nanjing 210023, People's Republic of China

[2] Key Laboratory of Drug Target and Drug for Degenerative Disease, Nanjing University of Chinese Medicine, Nanjing 210023, People's Republic of China

[3] Department of Biochemistry and Molecular Biology, Jiangsu Key Laboratory of Therapeutic Material of Chinese Medicine, School of Medicine and Life Science, Nanjing University of Chinese Medicine, Nanjing 210023, People's Republic of China

IκB-α	NF-kappa-B inhibitor alpha
IKK	Nuclear factor NF-kappa-B inhibitor kinase
LPS	Lipopolysaccharide
mRNA	Messenger RNA
mTOR	Mammalian target of rapamycin
mTORC	Mammalian target of rapamycin complex
NF-κB	Nuclear factor kappa-light-chain-enhancer of activated B cells
NIK	NF-kappa-B-inducing kinase
PAMPs	Pathogen-associated molecular patterns
PBS	Phosphate-buffered saline
RAI14	Retinoic acid-induced protein 14
Raptor	Regulatory-associated protein of mTOR
RT-qPCR	Quantitative real-time polymerase chain reaction
si-NC	Control siRNA.
siR-RAI14	RAI14 siRNA
siRNA	Small interfering RNA
TLRs	Toll-like receptors
TNF-α	Tumor-necrosis factor-α

Introduction

The human novel retinal pigment epithelial cell gene (NORPEG, RAI14) is a developmentally regulated gene originally derived from the human retinal pigment epithelial cell line, ARPE-19 (Kutty et al. 2001). This gene encodes the RAI14 protein that contains six ankyrin repeats and an extended coiled-coil domain. Moreover, RAI14 is widely expressed in a variety of human tissues and participates in the reorganization of actin filaments in the testis, contributing to spermatid polarity and cell adhesion (Chen et al. 2018a, b; Peng et al. 2000; Qian et al. 2013). While the Gene Ontology has deduced that RAI14 is associated with NIK/NF-κB signaling (Huttlin et al. 2017), the function of RAI14 in glial inflammation remains unknown.

It has been well established that the NF-κB signaling pathway is involved in the wide variety of pathological conditions, such as cancer and neurodegenerative diseases (Collignon et al. 2018; Li et al. 2012). Under different pathological conditions (e.g., LPS, TNF-α and hypoxia), NF-κB p65 activation and nuclear translocation control various transcriptional responses (Li et al. 2016). Thus, pro-inflammatory agonists, such as LPS and TNF-α, could play a vital role in the progression of diseases of the central nervous system. Additionally, since hypoxia can trigger a pro-inflammatory immune response (Cosin-Roger et al. 2017; Subhan et al. 2017), $CoCl_2$ (cobalt chloride), a hypoxia-mimetic agent, can be used to make an analogical analysis of the NF-κB inflammatory signaling pathway under conditions of chemical hypoxia. It has previously been shown that mTOR is associated with proinflammatory immune responses through the activation of the mTOR/IκB-α/NF-κB pathway (Temiz-Resitoglu et al. 2017). Moreover, the mammalian target of rapamycin (mTOR) functions as a serine/threonine protein kinase and controls protein synthesis, contributing to the associated physiological and pathological outcome (Caccamo et al. 2018; Wendel et al. 2004). mTOR is commonly comprised of mTOR complexes 1 (mTORC1) and 2 (mTORC2). In addition, mTORC1 activity is primarily inhibited by everolimus (RAD001) (Han et al. 2016; Yun et al. 2016), which has been shown to effectively treat cancers and autoimmune diseases (Kingwell 2013; Vitiello et al. 2015). Nevertheless, the precise molecular mechanisms underlying mTORC1-mediated inflammatory stress have yet to be sufficiently identified.

In the present study, we have explored the mechanisms underlying the RAI14 in mTOR-mediated inflammation using models of inflammation and chemical hypoxia.

Methods

Cell Culture and Treatment

The human glioma cell (U87) or human umbilical vein endothelial cell (HUVEC) was obtained from the American Type Culture Collection (ATCC, Manassas, VA, USA). U87 and HUVEC cells were cultured in Dulbecco's Modification of Eagle's Medium (DMEM; Gibco, Carlsbad, CA, USA) supplemented with 10% (v/v) fetal bovine serum (Gibco), 100 U/mL penicillin and 100 μg/mL streptomycin (Gibco). The cells were cultured in 60-mm culture dishes at 37 °C in a humidified atmosphere of 5% CO_2. U87 cells were grown on 60-mm culture dishes then incubated with 20 nM everolimus (MedChem Express, Monmouth Junction, NJ, USA) with or without TNF-α, LPS, or $CoCl_2$ as a baseline for further research. Recombinant human TNF-α was obtained from Hangzhou Biologic Biotechnology (China). All cell experiments were repeated at least three times.

Antibodies

Rabbit anti-RAI14 polyclonal antibody, rabbit anti-GAPDH polyclonal antibody, mouse anti-α-tubulin monoclonal antibody, rabbit anti-phospho-mTOR (Ser2448) antibody and rabbit anti-phospho-eIF4EBP1 (Thr37 + Thr46) antibody were purchased from Bioss (Beijing, China). Phospho-IKKα/β (Ser176/180) antibody and NF-κB p65 rabbit monoclonal antibody were obtained from Beyotime (Shanghai, China). Rabbit anti-α-actin monoclonal antibody, rabbit anti-β-actin polyclonal antibody, and rabbit anti-β-tubulin monoclonal antibody were obtained from BOSTER (Wuhan, China). All secondary antibodies were purchased from ZSGB-BIO (Beijing, China).

siRNA Transfection

The siRNA probe s25049 for RAI14, siRNA probe s25048 for RAI14 (Hasson et al. 2013), GAPDH positive control oligonucleotides and its control small interfering RNA (siRNA) in experiments refer to an All-Starnon silencing siRNA synthesized by Shanghai GenePharma (Shanghai, China). Lipo6000™ Transfection reagent (Beyotime) was used for the transfection of siRNA according to the manufacturer's instructions.

Quantitative Real-Time Polymerase Chain Reaction

A Reverse Transcription Kit and the SYBR Green PCR Master Mix were obtained from Takara (Otsu, Shiga, Japan). Total RNA was isolated from the cells using Trizol reagent according to the manufacturer's instructions (Beyotime) and cDNA was reverse-transcribed using a Reverse Transcription Kit (TaKaRa, Otsu, Shiga, Japan) according to the manufacturer's instructions. Real-time polymerase chain reaction (PCR) was performed using a QuantiTect SYBR Green PCR Kit (TaKaRa Bio), and run on a Stratagene MX3000P (Agilent, CA, USA). Relative quantification was determined using the $\Delta\Delta C_t$ method. The relative expression of messenger RNA (mRNA) for each gene was normalized to the level of β-actin RNA. The primers were synthesized by Invitrogen.

Western Blot

Cells were harvested and lysed in RIPA lysis buffer (Beyotime) supplemented with 1 mM phenylmethylsulfonyl fluoride. The protein concentration was determined using a BCA kit (Beyotime). An equal amount of each protein sample was separated on 10% or 8% sodium dodecyl sulfate–polyacrylamide electrophoresis gels and then transferred to a nitrocellulose filter membrane (Millipore, Solarbio, Beijing, China). Subsequently, the membranes were blocked for 1 h at room temperature with 5% BSA in TBST and incubated with the corresponding primary antibody overnight at 4 °C: rabbit anti-RAI14 polyclonal antibody (1:500), rabbit anti-phospho-IKKα/β (Ser176/180) antibody (1:1000), NF-κB p65 rabbit monoclonal antibody (1:000), rabbit anti-β-tubulin monoclonal antibody (1:300), mouse anti-α-tubulin monoclonal antibody (1:800), rabbit anti-β-actin polyclonal antibody (1:1000), rabbit anti-GAPDH polyclonal antibody (1:4000), and rabbit anti-α-actin monoclonal antibody (1:300). After washing with TBST thrice, the membranes were incubated with horseradish peroxidase-conjugated secondary antibodies anti-mouse IgG (1:10,000) or anti-rabbit IgG (1:10,000). The intensity of the protein bands was evaluated using an ECL Western Bot analysis kit (Millipore) and were normalized to those of α-actin or β-actin or α-tubulin or β-tubulin or GAPDH.

Co-immunoprecipitation

According to the manufacturer's instructions, 2 μg NF-κB p65 rabbit monoclonal antibody was added to the same amount (500 μg) of cell lysate overnight at 4 °C. Protein A/G-agarose spheres (Santa Cruz Biotechnology, Dallas, TX, USA) were added and the samples stored at 4 °C for 2 h. The samples were then centrifuged at 13,000*g* at 4 °C for 1 min, washed three times with lysis buffer, and boiled for 10 min after the addition of 30 μL 1× SDS Loading Buffer. The denatured samples were kept at − 20 °C for future western blotting.

Immunofluorescence Analysis

U87 cells were subjected to an immunofluorescence analysis following transfection and pharmaceutical treatment. An immunofluorescence analysis was used to observe the subcellular localization of the RAI14 protein and NF-κB p65 using a rabbit anti-RAI14 polyclonal antibody (1:300) or NF-κB Activation Nuclear Translocation Assay Kit according to the manufacturer's instructions (Beyotime). The protein levels of p-mTOR and p-eIF4EBP1 were performed using special antibodies, respectively. Cell nuclei were visualized by DAPI (40, 6-diamidino-2-phenylindole) staining. Fluorescence analysis was performed using a Leica DMi8S microscope (Leica Microsystems).

Cell Viability Assay

Cell viability was assessed using a Cell Counting Kit-8 (CCK-8) assay in accordance with the manufacturer's instructions. The CCK-8 kit was purchased from MedChem Express (Monmouth Junction, NJ, USA). The cells were plated at a density of 8×10^3 cells per well into 96-well plates. At 48 h after seeding, the cells were treated with different concentrations of LPS or TNF-α and transfected with siRNA. After culturing the cells for 24 h, 10 μL CCK-8 reagent was added to the medium. The cells were incubated for 4 h at 37 °C. A BioTek-Elx800 microplate reader (BioTek, Winooski, VT, USA) was used to measure the absorbance at 450 nm to assess cell viability.

Reactive Oxygen Species (ROS) Analysis

The U87 cellular ROS level was determined by ROS assay kit in accordance with the manufacturer's instructions (Beyotime). Briefly, U87 cells were treated with TNF-α for 24 h before DCFH-DA solution (10 μM) was added and then

incubated at 37 °C for 20 min. After washing the cells with serum-free medium, the sample was analyzed using a Leica DMi8S microscope (Leica Microsystems). Rosup was used as positive control.

Dual Luciferase Assay to Measure NF-κB Activity

According to the manufacturer's instructions, the NF-κB-dependent reporter constructs pNFκB-luc or pGL6 (Beyotime) were transiently transfected into U87 cells cultured in 24-well plates, using Lipo6000™ Transfection Reagent. The RL-SV40-N plasmid encoding Renilla luciferase (Beyotime) was simultaneously transfected as an internal control. After transfecting for 6 h, the cells were treated with 200 nmol/L LPS for 6 h and harvested using a Dual-Luciferase Reporter Gene Assay Kit (Beyotime) in accordance with the manufacturer's protocol. SpectraMax i3x was used to determine the results (Molecular Devices, CA, USA).

Statistical Analysis

At least three independent experiments were performed for each experiment. Data are presented as the mean ± SEM. Statistical analyses were performed using SPSS 22.0 (SPSS, Chicago, IL, USA). Analysis of variance and a Student's *t* test were used to compare the values of the test and the control samples. A one-way analysis of variance for a between–between design was used to analyze the differences between both time and condition and any interaction effect between the two. Statistical significance was considered if $P \leq 0.05$.

Results

Pro-inflammatory Agonists Induced the Elevation of RAI14 mRNA and Protein Levels in U87 Cells

RAI14 is a developmentally regulated gene induced by retinoic acid (Kutty et al. 2001). To assess the ability of the selected pro-inflammatory agonists to induce RAI14 mRNA and protein expression in U87 cells, RT-qPCR and western blotting were used to measure the level of RAI14 expression across different the time points in response to LPS (50, 100, and 200 ng/mL) or TNF-α (5, 10, 20, and 50 ng/mL) stimulation (Fig. 1; Table 1). Quantification of RAI14 mRNA and protein levels was performed at 6, 12, and 24 h following LPS treatment, and after 24 h and 48 h of TNF-α exposure. Each pro-inflammatory agonist spatially and temporally resulted in the elevation of RAI14 at the mRNA level (Fig. 1a, d). A more potent effect was evoked by LPS compared with TNF-α-treated U87 cells. There were

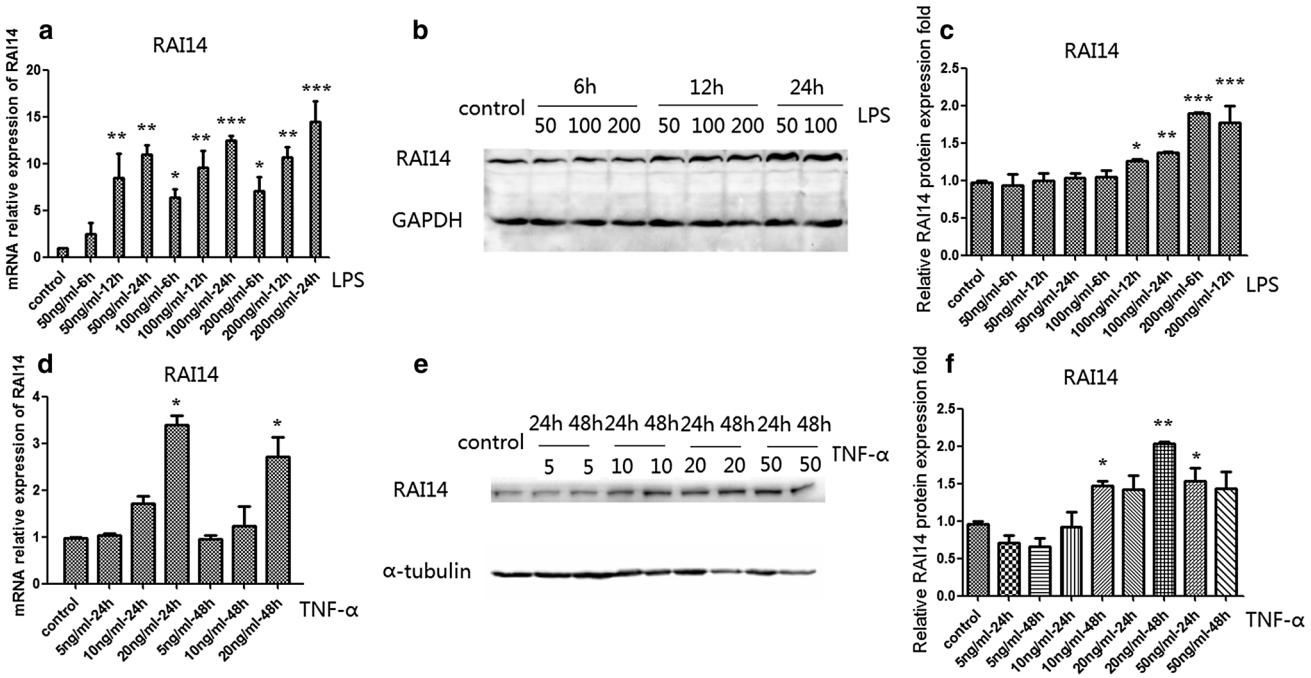

Fig. 1 Pro-inflammatory agonists induce elevated levels of RAI14 mRNA and protein expression in U87 cells. U87 cells were incubated for 6, 12, 24, or 48 h in the presence of PBS (control), LPS (50, 100, and 200 ng/mL), or TNF-α (5, 10, 20, and 50 ng/mL) for the subsequent quantification of RAI14. LPS (**a**–**c**) and TNF-α (**d**–**f**) spatially and temporally increased the level of RAI14 mRNA and protein expression. Data are displayed as the mean ± SEM. $^{*}P < 0.05$, $^{**}P < 0.01$, and $^{***}P < 0.001$ compared with the control groups

Table 1 Primer sequences used for RT-qPCR measurements

Target gene	Forward and reverse primer sequences (5′-3′)	NCBI reference
RAI14	Forward: AATGCAGGAATTCAAAGCCTTCTATT Reverse: GGTAGGACTGATAGGAGGTGG	NM_001145520.1
GADPH	Forward: ATCACCATCTTCCCAGGAGCG Reverse: AGTTGGTGGTGCAGGAGG	NM_002046.6
ACTB	Forward: CCCAGCACAATGAAGATCAAGAT Reverse: GGACTCGTCATACTCCTGCTT	NM_001101.4
IL1B	Forward: GGCCCTAAACAGCTGAAGTGC Reverse: CATGGCCACAACAACTGACG	NM_000576.2
TNFα	Forward: AGCCCATGTTGTAGCAAACC Reverse: CTGATGGTGTGGGTGAGGAG	NM_000594.3
IL6	Forward: CAATCTGGATTCAATGAGGAGAC Reverse: CATTTGTGGTTGGGTCAGGG	NM_000600.4

significant 190% ($P < 0.001$) and 203% ($P < 0.001$) increases in the protein expression of RAI14, induced by 200 ng/mL LPS for 6 h and 20 ng/mL TNF-α for 48 h, respectively (Fig. 1c, f). Thus, the RAI14 appears to be regulated by pro-inflammatory agonists, particularly LPS.

Effect of RAI14 Knockdown on Pro-inflammatory Cytokine mRNA Expression Under Pro-inflammatory Conditions

To date, there have been no published reports regarding the effect of RAI14 on pro-inflammatory cytokine production in astrocytes. Thus, to elucidate this effect, we targeted RAI14 in U87 cell cultures. After an RAI14 knockdown (Fig. 2a–d), a significant decrease in RAI14 protein and mRNA expression was observed (38.1% and 38.7%, respectively). To quantify the induction of pro-inflammatory cytokine mRNA expression in response to TNF-α exposure, RT-qPCR was used to measure the level of IL-1β and IL-6 mRNA expression. A predefined dose of 20 ng/mL TNF-α was shown to significantly promote inflammation in comparison to the control groups (Fig. 2e, f). The highest induction of IL-1β (267.2%) was observed at 48 h, and the level of IL-6 mRNA was significantly elevated at 48 h (199.7%). However, the depletion of RAI14 in U87 cell lines resulted in an attenuation of TNF-α-induced inflammation (Fig. 2g, h). These findings indicate that RAI14 positively regulates the expression of pro-inflammatory cytokines in response to LPS and TNF.

RAI14 Knockdown Attenuates Pro-inflammatory Agonist-Induced NF-κB Activation

Through the process of Gene Ontology, RAI14 is considered to be associated with NIK/NF-κB signaling (Huttlin et al. 2017). This is consistent with the observed direct association of siR-RAI14-mediated proinflammatory cytokine responses (Fig. 2g, h). To explore the precise mechanism by which RAI14 regulates proinflammatory cytokines, immunofluorescence microscopy was used to investigate the potential effect of an RAI14 knockdown on NF-κB p65 activation in U87 cells. The level of p65 intensity in the nuclei of TNFα-stimulated U87 cells was increased compared with the controls (Fig. 3a). Moreover, siR-RAI14 treatment was associated with decreased NF-κB p65 in the nuclei of the stimulated cells decreased compared to the corresponding siR-NC (Fig. 3b), indicating RAI14 could promote the nuclear accumulation of p65. In addition, we observed a partial inhibition of NF-κB p65 activation and nuclear translocation with the use of a nanoparticle transfection reagent to carry the siRNA (Online Resource 1). Although RAI14 was found to partially co-localize with NF-κB p65 in the nucleus and the cytoplasm (Fig. 3b), no structural association between endogenous RAI14 and NF-κB p65 was detected by Co-IP (Fig. 3c).

Since RAI14 has been suggested to attach to predicted transcription factors and cofactors in the human genome (Li et al. 2008), we next analyzed whether RAI14 effects the NF-κB signaling pathway in U87 cells expressing a Firefly luciferase reporter gene driven by a promoter containing an NF-κB response element. U87 cells were co-transfected with pNFκB-luc or pGL6 (empty vector), along with pRL-SV40-N constitutively expressing the Renilla luciferase, as an internal control for data normalization. Cells were exposed to 200 ng/mL LPS for 6 h to establish a baseline for further research. The inhibition of RAI14 substantially blocked Firefly luciferase activity, whereas transfection with the pGL6 vector only exhibited a moderate effect on luciferase activity (Fig. 3d), suggesting that RAI14 is involved in the regulation of the positive response for pro-inflammatory cytokines via NF-κB signaling.

Everolimus Inhibits the RAI14 Transcription–Translation Reaction and Ameliorates Inflammatory Activity

RAI14 has been found to exhibit a significant correlation with everolimus (Hsu et al. 2013), an mTOR inhibitor,

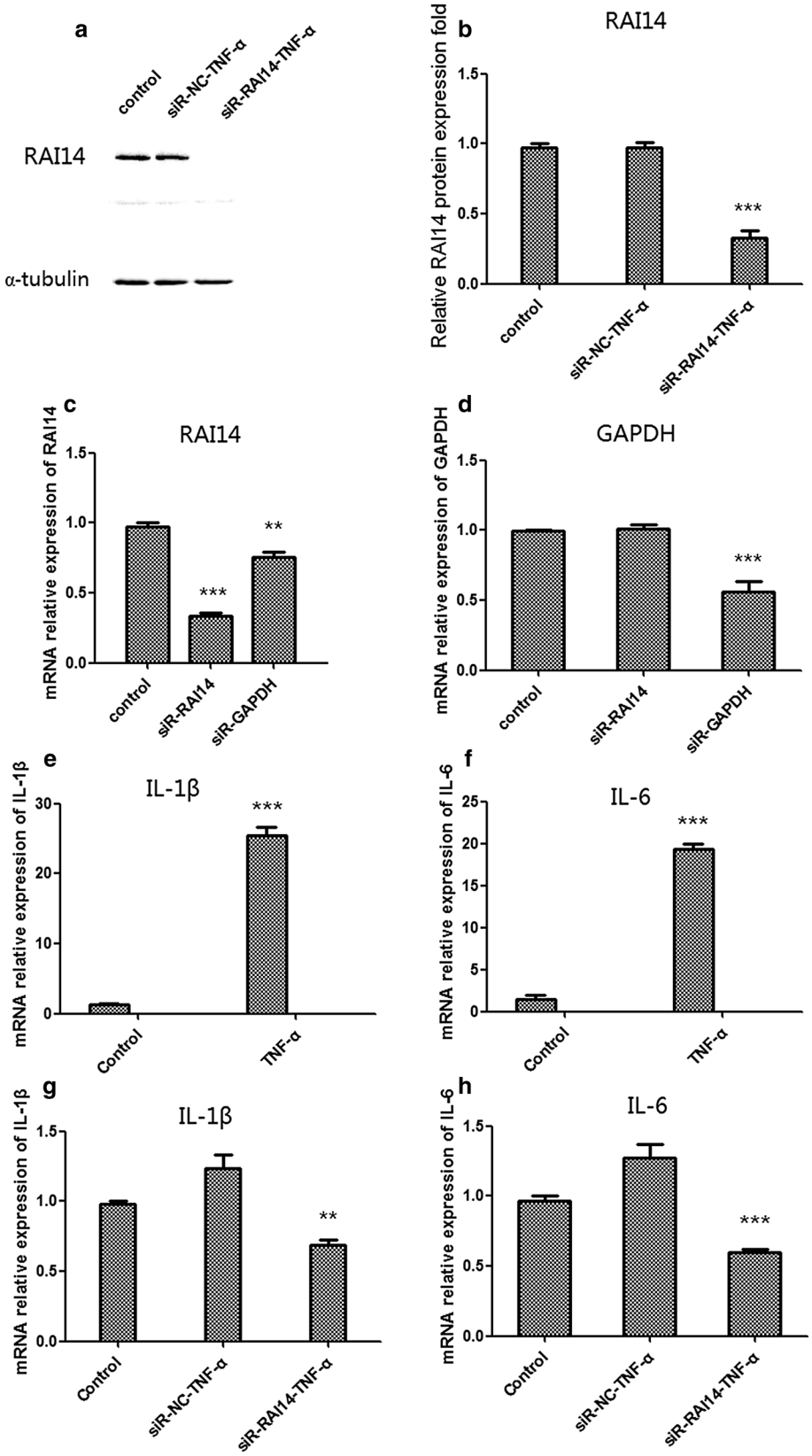

Fig. 2 Effect of siR-RAI14 on pro-inflammatory cytokine mRNA expression in response to 20 ng/mL TNF-α. U87 Cells were transfected with siRNA against RAI14 (*siR-RAI14*) or GAPDH (*siR-GAPDH*) or a Lipo6000™ Transfection reagent (*control*) as indicated. **a**–**d** After the knockdown of RAI14, the level of RAI14 protein or mRNA expression was measured by western blot (**a**, **b**) and RT-qPCR (**c**, **d**), respectively. **e**, **f** Effect of TNF-α on IL-1β and IL-6 genes expressed in U87 cells by RT-qPCR. **g**, **h** Effect of siR-RAI14 on IL-1β and IL-6 genes expressed in U87 cells exposed to TNF-α by RT-qPCR. Data are displayed as the mean ± SEM. $^{*}P < 0.05$, $^{**}P < 0.01$, and $^{***}P < 0.001$ compared with the control groups

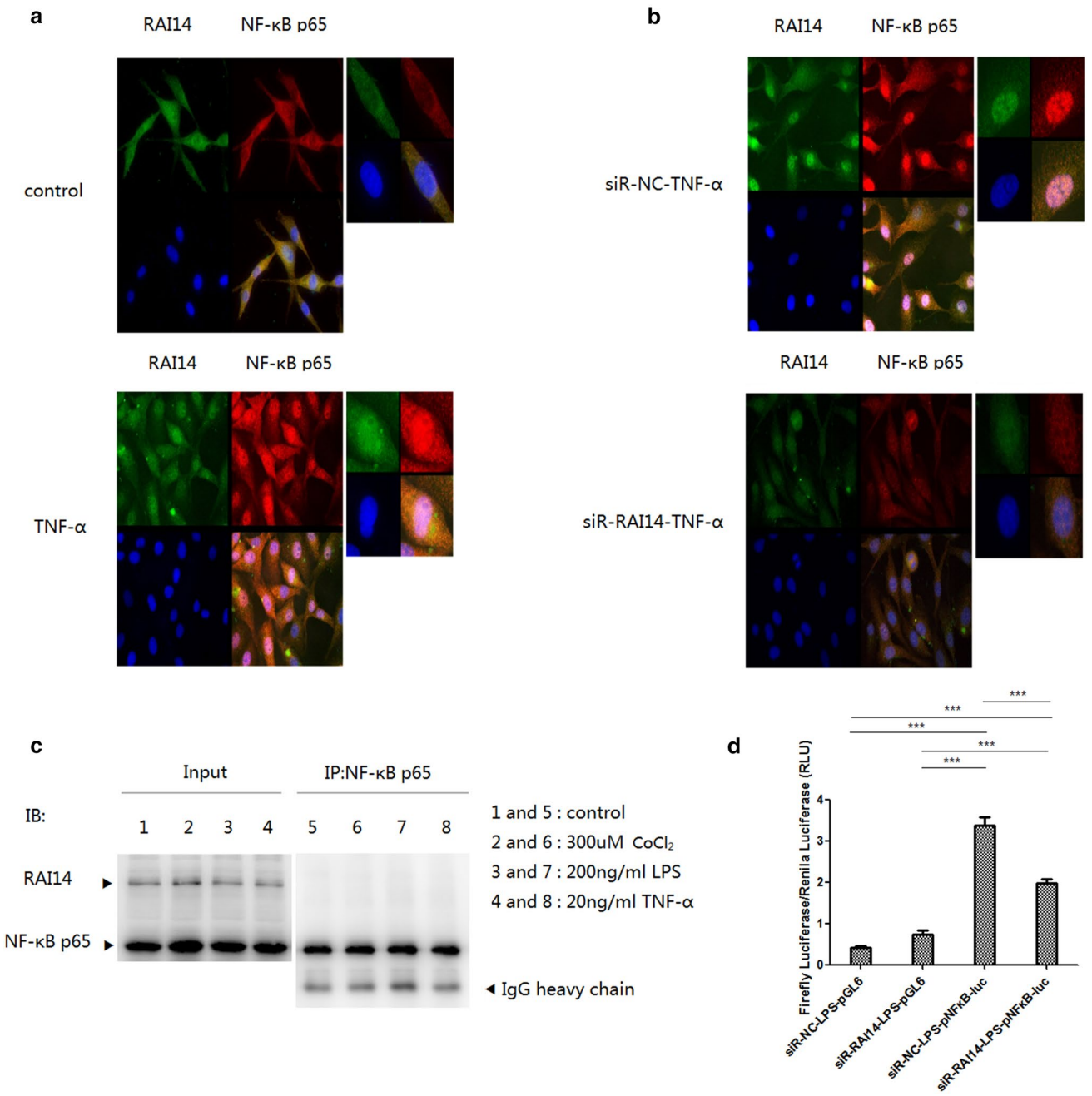

Fig. 3 RAI14 knockdown attenuates pro-inflammatory agonist-induced NF-κB activation. **a** The effect of TNF-α on the nuclear translocation of NF-κB transcription factor p65. **b** Inhibition of RAI14 prevented the nuclear accumulation of NF-κB p65. Immunofluorescence analysis of the fields of NF-κB p65 and RAI14 localization using anti-NF-κB p65 (red) and anti-RAI14 (green) in U87cells in response to stimulation with 20 ng/mL TNF-α for 48 h. Cell nuclei were stained with DAPI (blue). *Scale bar* 20 μm. **c** The inability of RAI14 to directly bind to NF-κB p65. U87 cells were harvested and lysed after exposure to a variety of stimuli. RAI14 did not structurally interact with NF-κB p65 in the intracellular environment. **d** siR-RAI14 can promote the activation of an NF-κB dependent reporter. After siRNA transfection, U87 cells were co-transfected with the NF-κB dependent reporter construct pNFκB-luc, pRL-SV40-N-Renilla luciferase, or pGL6. Cells were then stimulated with 200 ng/mL LPS for 6 h. Firefly luciferase activity was normalized against Renilla luciferase activity. Values are expressed as the mean ± SEM of three independent experiments

which exerts a potent influence on anti-inflammatory activity (Vitiello et al. 2015). To determine the effect of everolimus on RAI14 during the inflammatory response, western blot was performed to analyze the expression of RAI14 protein. After 24 h incubation with everolimus, the U87 cells displayed reduced expression of total RAI14 protein

(Fig. 4a–d). Although everolimus inhibited the production of RAI14 protein, no significant differences were observed for the effect of everolimus (20 nM) on the level of RAI14 mRNA in the LPS-induced inflammation model (Fig. 4e). Using an mTOR inhibitor, we also observed a significant inhibitory effect of everolimus regarding the level of IL-1β and IL-6 mRNA evoked by LPS (Fig. 4f, g), consistent with studies of Vitiello et al. (2015). Everolimus treatment also inhibited protein levels of p-mTOR but increased protein levels of p-eIF4EBP1 in response to TNF-α stimuli (Fig. 4h, i). These data suggest that mTOR/eIF4EBP1 signaling is involved in the RAI14 transcription-translation reaction in astrocytes.

Everolimus Ameliorates NF-κB Activity and IKKα/β Phosphorylation in a RAI14-Dependent Manner

Since everolimus was found to be involved in inhibiting RAI14 and inflammatory activity (Fig. 4), we next sought to determine the influence of an RAI14 knockdown on everolimus-mediated pro-inflammatory cytokine inhibition by measuring the level of IL-1β, IL-6, and TNF-α expression with RT-qPCR. Following siR-RAI14 transfection, IL-1β, IL-6, and TNF-α were observed to be consistently expressed at a lower level than the corresponding controls when the same amount of siR-NC was transfected (Fig. 5a). Since: (1) the RT-qPCR data showed that

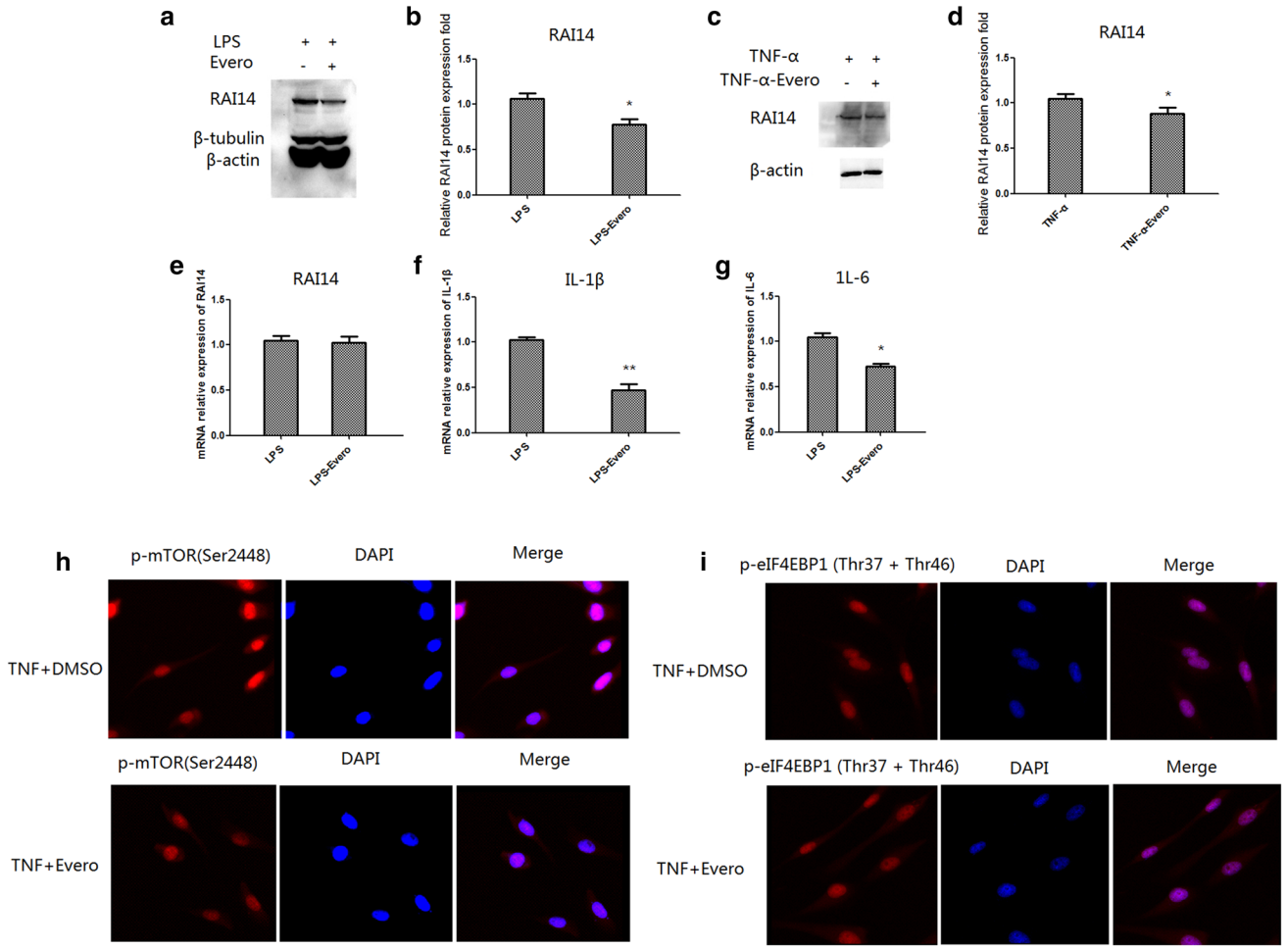

Fig. 4 Everolimus inhibited the RAI14 transcription–translation reaction and ameliorated inflammatory activity. **a–d** Before treatment with everolimus (20 nM), U87 cells were exposed to LPS (200 ng/mL) for 6 h (**a**) or TNF- α (20 ng/mL) for 48 h (**b**) and the level of RAI14 protein expression was analyzed. **a**, **c** Western blots of RAI14 protein were compared to β-tubulin or/and β-actin standards. **c**, **d** Quantitation of western blots for RAI14 protein expression. **e** Effect of everolimus (20 nM) exposure on mRNA levels for RAI14 in U87 cells following LPS stimulation, as measured by RT-qPCR. **f**, **g** Levels of inflammatory cytokine mRNA from U87cells cultured with everolimus (20 nM) for 24 h. Levels of the pro-inflammatory cytokines, IL-1β and IL-6, decreased in the everolimus-treated groups. Protein levels of p-mTOR (**h**) and p-eIF4EBP (**i**) from U87cells cultured with everolimus (20 nM) for 24 h. Values show the mean ± SEM of three independent experiments with similar results.*$P < 0.05$ and **$P < 0.01$. Everolimus was dissolved in DMSO and the equivalent volume of DMSO was added to the corresponding controls. *LPS* lipopolysaccharide, *DMSO* phosphate-buffered saline, *TNF-α* tumor-necrosis factor-a, *RAI14* retinoic acid-induced protein 14, *evero* everolimus

everolimus ameliorated inflammatory activity and inhibited the RAI14 transcription-translation reaction (Fig. 4); (2) TNF-α and LPS have been shown to regulate mTOR activity via IKKβ (Lee et al. 2007) and NF-κB activity may be controlled by mTOR in a cell type-specific manner (Guo et al. 2013); and (3) our dual luciferase assay data demonstrated that siR-RAI14 induced the downregulation of luciferase activity under the control of the NF-κB p65 promoter (Fig. 3d), we next sought to investigate the molecular mechanisms underlying the effect of everolimus on the relationship between RAI14 and NF-κB signaling. To this end, we used siR-RAI14 to analyze the downregulation of pro-inflammatory cytokines in the everolimus-treated groups. Consistent with the role of mTOR/Raptor in positively regulating NF-κB activity (Dan et al. 2008), we observed decreased NF-κB p65 protein expression (Fig. 5b, d) and decreased IKKα/β phosphorylation (Fig. 5f) following everolimus treatment. Importantly, transfection with siR-RAI14 further strengthened the effects of the mTOR inhibitor on the negative regulation of NF-κB p65 (Fig. 5b, d). Similarly, a knockdown of RAI14 substantially enhanced the downregulation of everolimus-mediated p-IKKα/β (Fig. 5f). These observations suggest that mTOR activity may be a strong promoter of the RAI14-mediated positive regulation of the NF-κB signaling pathway.

Inhibitory Effect of Everolimus on $CoCl_2$-Induced Astrocyte Inflammation Related with RAI14

Due to the effects of hypoxia on triggering pro-inflammatory responses (Cosin-Roger et al. 2017; Subhan et al. 2017), $CoCl_2$, a hypoxia-mimetic agent, was used to make an analogical analysis of the role of the mTOR/RAI14 signaling pathway on the astrocyte inflammatory reaction derived from chemical hypoxia. Following incubation with 50, 100, 300, or 500 μM $CoCl_2$ for 24 h, U87 cells were lysed to monitor the level of RAI14 protein expression. As expected, 50 μM $CoCl_2$ resulted in a reduced expression of the total RAI14 protein, while 100 μM $CoCl_2$ resulted in the barely detectable quantification of RAI14 protein levels in U87 cells (Fig. 6a). Most importantly, this influence could be reversed by treatment with 300 or 500 μM $CoCl_2$ (Fig. 6b). Consistent with this observation, the impact of $CoCl_2$ on IL-6 and TNF-α gene expression exhibited a similar effect in U87 cells during the same period (Fig. 6c, d). Similarly, in our model of hypoxia, everolimus was observed to be an effective negative regulator of NF-κB p65, which was further strengthened following transfection with siR-RAI14 (Fig. 6e, f). These results provide further insight into the role of RAI14 on mTOR-mediated NF-κB inflammatory signaling under conditions of chemical hypoxia.

Discussion

The central nervous system can launch a series of innate immune responses under both infectious and noninfectious conditions. In general, astrocytes and microglia participate in this innate immune response through the release of proinflammatory cytokines and chemokines, as well as the induction of phagocytosis and cytotoxicity, ultimately resulting in neuroinflammation (Guo et al. 2018; Kielian 2006; Liu et al. 2017). The immediate activation of resident glial cells via Toll-like receptors (TLRs) in response to the recognition of diverse pathogen-associated molecular patterns (PAMPs) maximize proinflammatory responses within the CNS. In this study, we used LPS- and TNF-α as stimuli and found that both could spatially and temporally regulate the level and functionality of RAI14 (Fig. 1). In addition, a knockdown of RAI14 significantly ameliorated the inflammatory response in astrocytes (Fig. 2), which is consistent with the suggestion that RAI14 is associated with NIK/NF-κB signaling (Huttlin et al. 2017).

It has been well established that the expression of NF-κB-dependent genes is involved in the pathological course of conditions, such as inflammatory stress and neurodegenerative diseases (Li et al. 2012). Indeed, the activation and nuclear translocation of NF-κB via TLR signaling controls the expression of a wide array of genes related to the immune response (Kielian 2006). In our analysis of the effect of RAI14 on NF-κB p65, we found that the knockdown of RAI14 greatly diminished NF-κB p65 activation and nuclear translocation and actively blocked the transcription of the Firefly luciferase reporter gene driven by a promoter containing the NF-κB response element (Fig. 3). Although the co-localization of RAI14 with NF-κB p65 was observed via immunofluorescence microscopy, and there is a substantial similarity in the sequences and structure of the ankyrin repeat domain between IκBα (69–282 aa) and RAI14 (12–270 aa) (Online Resource 2), no structural association between endogenous RAI14 and NF-κB p65 was detected in our Co-IP assay (Fig. 3). Since the RAI14 protein contains six ankyrin repeats and an extended coiled-coil domain, we assumed that the coiled-coil domain has an inhibitory function when interacting with the ankyrin repeat domain when there is no activation signal. Moreover, there is a binding site sequence for the classical masking of the 14-3-3 protein and the nuclear localization signal in the amino acid sequences of the RAI14 protein (Kutty et al. 2006). Since RAI14 can form a protein complex with its 14-3-3 binding partner (Huttlin et al. 2017), we deduced that this complex blocked the endogenous combination between RAI14 and NF-κB p65.

The mTOR pathway contributes to the physiological and pathological course of several processes, including

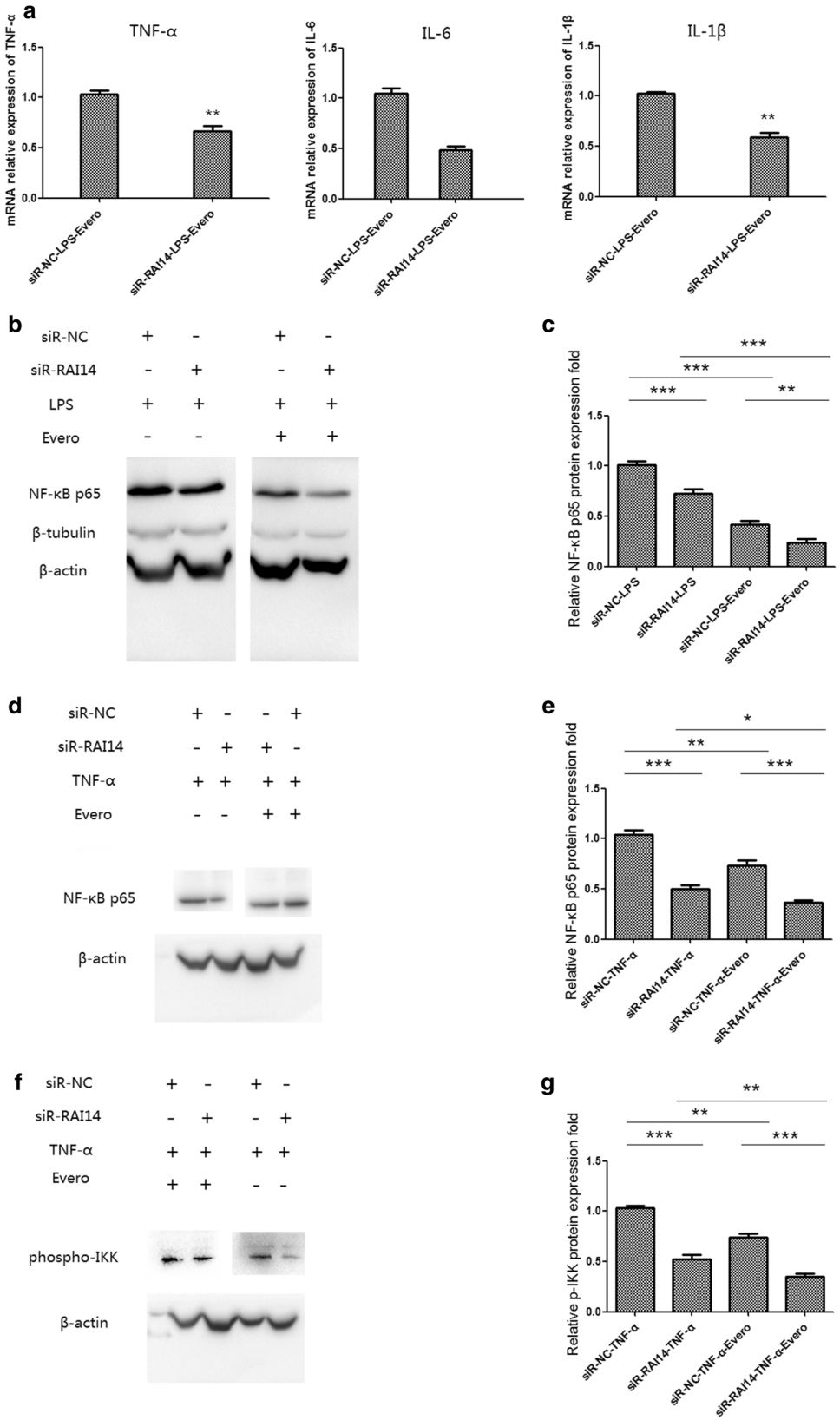

Fig. 5 Everolimus ameliorates NF-κB activity and IKKα/β phosphorylation in an RAI14-dependent manner. **a** U87 cells were pre-treated with LPS (200 ng/mL) for 6 h before plasmid transient transfection for 6 h. Levels of the pro-inflammatory cytokines, IL-1β, IL-6, and TNF-α, were quantified by RT-qPCR. **b**–**g** After transient transfection, U87 cells were exposed to LPS (200 ng/mL) for 6 h **b, c** or TNF-α (20 ng/mL) for 48 h **d**–**g** prior to everolimus (20 nM) treatment for 24 h. The level of p-IKKα/β(Ser176/180) and NF-κB p65 protein expression was analyzed. **b**, **d**, **f** Western blots of p-IKKα/β(Ser176/180) and NF-κB p65 protein expression were compared to β-tubulin or/and β-actin standards. **c**, **e**, **g** Quantitation of western blots of p-IKKα/β(Ser176/180) and NF-κB p65 protein. Everolimus was dissolved in DMSO and then diluted with appropriate media. The equivalent volume of DMSO was added to the corresponding controls. Values show the mean ± SEM of three independent experiments with similar results.*$P < 0.05$; **$P < 0.01$; and ***$P < 0.001$

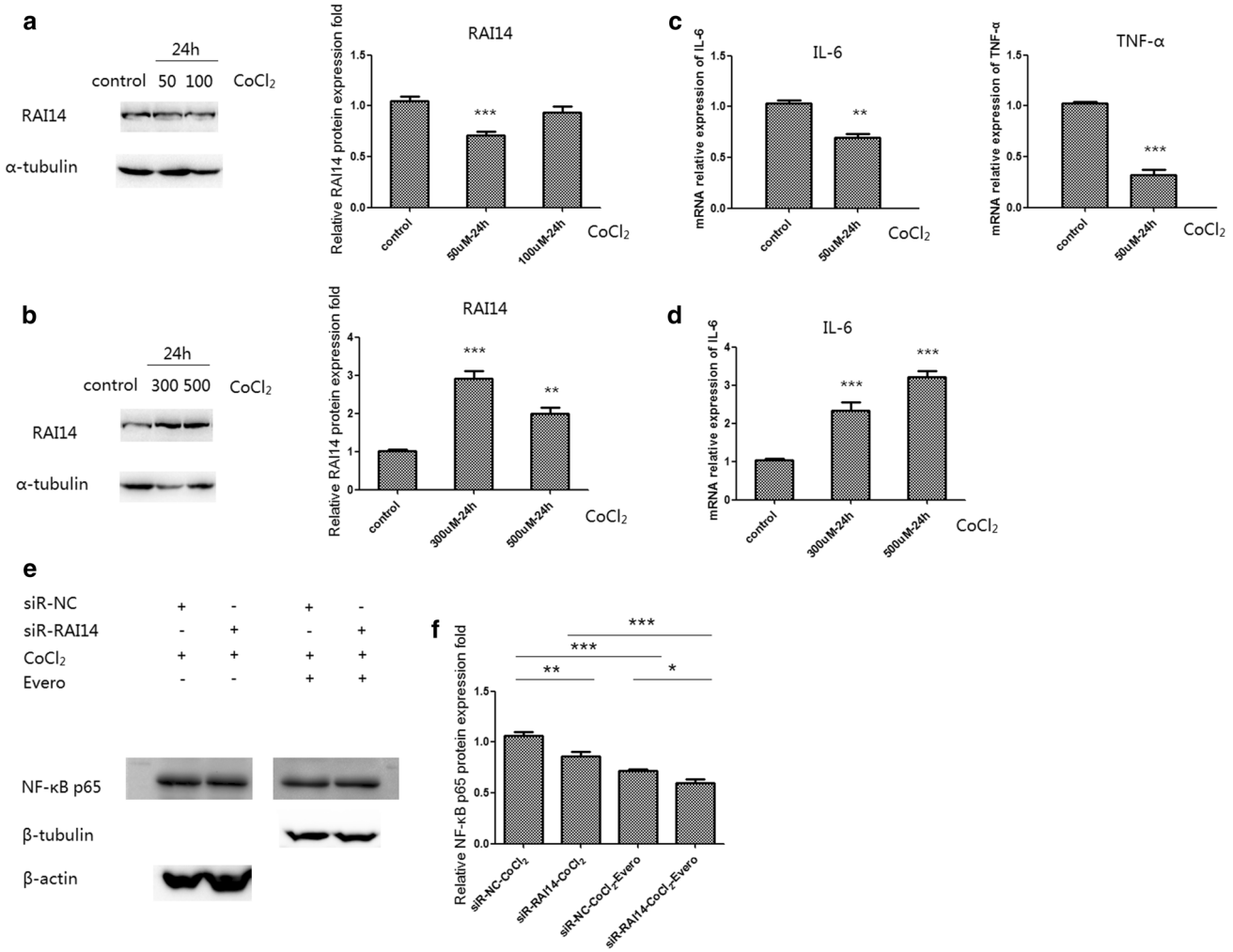

Fig. 6 Inhibitory effects of everolimus on $CoCl_2$-induced inflammation related with RAI14. **a**, **b** Decreased levels of RAI14 protein expression were induced by treatment with 50 μM $CoCl_2$ **a** but reversed by treatment with 300 or 500 μM $CoCl_2$ for 24 h (**b**). **c**, **d** Effect of $CoCl_2$ on IL-6 and TNF-α genes expression in U87 cells by RT-qPCR. **e**, **f** siR-RAI14-mediated decrease in the level of NF-κB p65 protein in U87 cells when exposed to $CoCl_2$ (300 μM) was significantly promoted by treatment with 20 ng/mL Evero for 24 h. Everolimus was dissolved in DMSO and then diluted with appropriate media. The equivalent volume of DMSO was added to the corresponding controls. Results are presented as the means ± SD of three independent experiments. *$P < 0\,05$; **$P < 0\,01$; and ***$P < 0\,001$

cell growth, survival, metabolism, cancer, and neurodegenerative diseases (Caccamo et al. 2018; Wendel et al. 2004). A previous study has shown that mTOR, a serine/threonine protein kinase, is associated with proinflammatory immune responses through the activation of the mTOR/IκB-α/NF-κB pathway (Temiz-Resitoglu et al. 2017). Moreover, TNF-α and LPS have been shown to regulate mTOR activity via IKKβ (Lee et al. 2007) and mTOR may control NF-κB activity in a cell type-specific manner (Guo et al. 2013). In addition, a significant correlation has been found between the RAI14 gene and everolimus (Hsu et al. 2013). Therefore, we sought to investigate the correlation between mTOR, RAI14, and NF-κB, as well as examine the impact of RAI14 on mTOR-mediated NF-κB signaling in astrocytes. Under everolimus-mediated downregulation of mTOR activation, we observed a marked decrease in the mRNA levels of IL-1β and IL-6 and reduced total RAI14 protein expression; however, there were no significant differences in the level of RAI14 mRNA expression during astrocyte inflammation (Fig. 4), suggesting the impact of active mTOR on the RAI14 transcription–translation reaction. Indeed, mTORC1 can mediate phospho-eukaryotic initiation factor 4E binding protein 1 (4EBP1) (Coffey et al. 2016; Hara et al. 1997), which dissociates from eukaryotic translational initiation factor 4 epsilon (eIF4E), leading to the initiation of translation (Hay and Sonenberg 2004). Previous studies have proved that mTORC1 plays a key role in mouse RAI14 mRNA translation, which was effectively inhibited in DKO (4E-BP1/2 double-knockout MEFs) cells compared to WT cells treated with Torin1

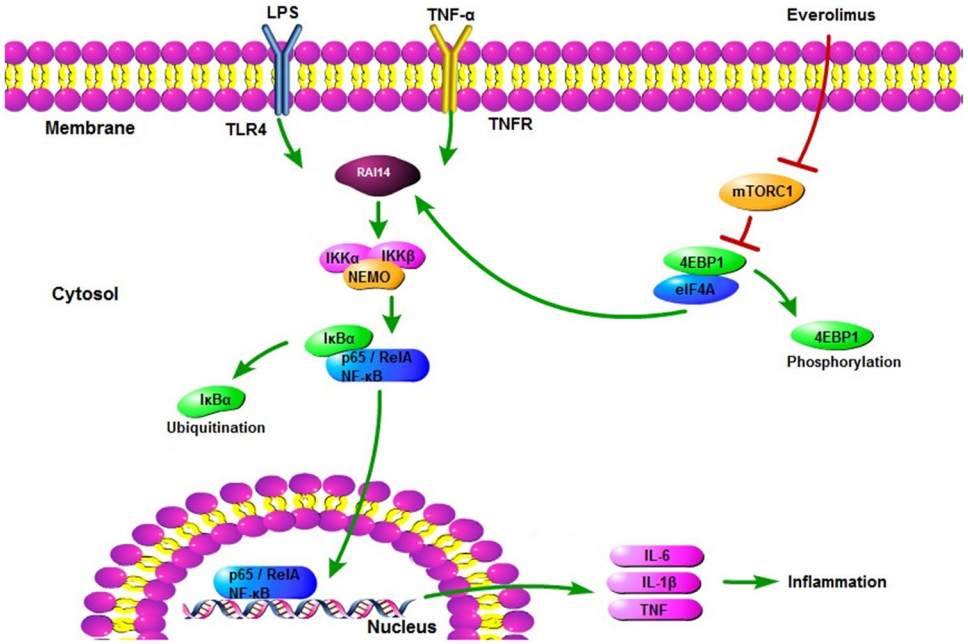

Fig. 7 A tentative model of RAI14 in inflammatory responses is shown schematically. Pro-inflammatory agonists, such as LPS and TNF-α, induce the expression of RAI14. Subsequently, RAI14 activation contributes to the positive regulation of IKKα/β phosphorylation and NF-κB activation and nuclear translocation, allowing for the subsequent induction of NF-κB-dependent genes, such as TNF-α, IL-6, and IL-1β. The serine/threonine protein kinase, mTORC1, is also involved in RAI14 activation. It likely controls the RAI14 transcription–translation reaction through the mTORC1/4EBP1/eIF4E signaling pathway

for 2 h (Thoreen et al. 2012). Our present data further suggests mTORC1-mediated RAI14 mRNA translation, especially in human cells (Fig. 4h, i). It is noteworthy that RAI14 transcript is more likely a TOP-like mRNA on account of the ~2-kb-long 3′-untranslated region of its transcript (Kutty et al. 2001).Thus, everolimus may inhibit the RAI14 transcription–translation reaction through the mTORC1/4EBP1/eIF4E signaling pathway. Notably, the RAI14 knockdown substantially enhanced the effects of the mTOR inhibitor-mediated downregulation of NF-κB p65, p-IKKα/β, and pro-inflammatory cytokines (e.g., TNF-α, IL-1β, and IL-6) (Fig. 5), suggesting that RAI14 contributed to mTOR-mediated NF-κB activation. Similarly, everolimus also ameliorated inflammatory activity via RAI14 in HUVEC cells (Online Resource 3). Thus, we propose a tentative model of RAI14 in inflammatory responses (Fig. 7). As for U87 cell proliferation, everolimus decreased ROS levels via RAI14 and effectively maintained normal cell morphology, suggesting that mTOR signaling may contribute to cell survival under inflammatory stress (Online Resource 4). However, no significant changes were observed following exposure to various stimulating factors in CCK-8 assays (Online Resource 5).

Since the interplay between RAI14, mTOR, and NF-κB tends to be complex, we used $CoCl_2$ to analogically analyze the role of RAI14 in mTOR-mediated inflammatory responses under conditions of chemical hypoxia. However, the influence of hypoxia on mTOR-mediated inflammation remains controversial. Under conditions of ischemic preconditioning, environmental hypoxia ameliorates inflammation through the downregulation of the mTOR-NLRP3 complex and the activation of autophagy (Cosin-Roger et al. 2017). In contrast, the expression of p-mTOR and activated autophagy may display coordinated regulation in cerebral ischemia/reperfusion lesions and chemical hypoxia-mediated the inflammatory response (Gu et al. 2013; Yang et al. 2015). In the present study, we demonstrated that different concentrations of $CoCl_2$ exerted an opposing influence on RAI14 and the glial inflammatory response (Fig. 6). Furthermore, the effect of mTOR on autophagy remains elusive. Indeed, mTOR has been shown to block autophagy in response to myocardial ischemia/reperfusion injury, and the mTOR activator, MHY1485, inhibits autophagy via blocking autolysosome formation (Chen et al. 2018a, b; Choi et al. 2012). Under the MHY1485-mediated upregulation of mTOR activity, we observed a marked increase in the level of RAI14 mRNA (Online Resource 6). Thus, RAI14 may be a critical intermediate in the relationship between mTOR, NF-κB, and autophagy. However, further research is required to verify this association.

Conclusions

The present study found a novel mechanism underlying the activation of NF-κB induced by mTOR signaling. RAI14 is the active intermediate responsible for increasing the effect of mTOR on NF-κB activation. Thus, the vital role of RAI14 in the inflammatory response could contribute to the treatment of inflammation-related central nervous system disorders and implies that RAI14 may be a potential drug target for the treatment of such diseases.

Author Contributions In this study, JG conceived the general idea. XGS, JRZ, XLZ, YFW, and YFH carried out experiments. XGS, and JG analyzed and interpreted the data and wrote the paper. JG critically reviewed and edited the work. All authors approved the final version of the manuscript.

Funding This work was supported by Grants from the National Natural Science Foundation of China (81573409) and Natural Science Foundation of Jiangsu Province (BK20161574) and A Project Funded by the Priority Academic Program Development of Jiangsu Higher Education Institutions (Integration of Raditional Chinese and Western Medicine).

Compliance with Ethical Standards

Conflict of interest The authors declare that they have no conflict of interest.

Ethical Approval This article does not contain any studies with human participants or animals performed by any of the authors. The manuscript does not contain clinical studies or patient data.

References

Caccamo A, Belfiore R, Oddo S (2018) Genetically reducing mTOR signaling rescues central insulin dysregulation in a mouse model of Alzheimer's disease. Neurobiol Aging 68:59–67. https://doi.org/10.1016/j.neurobiolaging.2018.03.032

Chen T, Guo Y, Shan J, Zhang J, Shen X, Guo J, Liu XM (2018a) Vector analysis of cytoskeletal structural tension and the mechanisms that underpin spectrin-related forces in pyroptosis. Antioxid Redox Sign. https://doi.org/10.1089/ars.2017.7366

Chen WR, Liu HB, Chen YD, Sha Y, Ma Q, Zhu PJ, Mu Y (2018b) Melatonin attenuates myocardial ischemia/reperfusion injury by inhibiting autophagy via an AMPK/mTOR signaling pathway. Cell Physiol Biochem 47:2067–2076. https://doi.org/10.1159/000491474

Choi YJ et al (2012) Inhibitory effect of mTOR activator MHY1485 on autophagy: suppression of lysosomal fusion. PLoS ONE 7:e43418. https://doi.org/10.1371/journal.pone.0043418

Coffey RT, Shi Y, Long MJC, Marr MTN, Hedstrom L (2016) Ubiquilin-mediated small molecule inhibition of mammalian target of rapamycin complex 1 (mTORC1) signaling. J Biol Chem 291:5221–5233. https://doi.org/10.1074/jbc.M115.691584

Collignon E et al (2018) Immunity drives TET1 regulation in cancer through NF-kappaB. Sci Adv 4:7309. https://doi.org/10.1126/sciadv.aap7309

Cosin-Roger J et al (2017) Hypoxia ameliorates intestinal inflammation through NLRP3/mTOR downregulation and autophagy activation. Nat Commun 8:98. https://doi.org/10.1038/s41467-017-00213-3

Dan HC, Cooper MJ, Cogswell PC, Duncan JA, Ting JP, Baldwin AS (2008) Akt-dependent regulation of NF-{kappa}B is controlled by mTOR and Raptor in association with IKK. Gene Dev 22:1490–1500. https://doi.org/10.1101/gad.1662308

Gu L, Huang B, Shen W, Gao L, Ding Z, Wu H, Guo J (2013) Early activation of nSMase2/ceramide pathway in astrocytes is involved in ischemia-associated neuronal damage via inflammation in rat hippocampi. J Neuroinflamm 10:109. https://doi.org/10.1186/1742-2094-10-109

Guo F et al (2013) mTOR regulates DNA damage response through NF-kappaB-mediated FANCD2 pathway in hematopoietic cells. Leukemia 27:2040–2046. https://doi.org/10.1038/leu.2013.93

Guo YC, Wang YX, Ge YP, Yu LJ, Guo J (2018) Analysis of subcellular structural tension in axonal growth of neurons. Rev Neurosci 29:125–137. https://doi.org/10.1515/revneuro-2017-0047

Han R, Gao J, Zhai H, Xiao J, Ding Y, Hao J (2016) RAD001 (everolimus) attenuates experimental autoimmune neuritis by inhibiting the mTOR pathway, elevating Akt activity and polarizing M2 macrophages. Exp Neurol 280:106–114. https://doi.org/10.1016/j.expneurol.2016.04.005

Hara K et al (1997) Regulation of eIF-4E BP1 phosphorylation by mTOR. J Biol Chem 272:26457–26463

Hasson SA et al (2013) High-content genome-wide RNAi screens identify regulators of parkin upstream of mitophagy. Nature 504:291–295. https://doi.org/10.1038/nature12748

Hay N, Sonenberg N (2004) Upstream and downstream of mTOR. Gene Dev 18:1926–1945

Hsu Y et al (2013) Genome-wide analysis of three-way interplay among gene expression, cancer cell invasion and anticancer compound sensitivity. BMC Med 11:106. https://doi.org/10.1186/1741-7015-11-106

Huttlin EL et al (2017) Architecture of the human interactome defines protein communities and disease networks. Nature 545:505–509. https://doi.org/10.1038/nature22366

Kielian T (2006) Toll-like receptors in central nervous system glial inflammation and homeostasis. J Neurosci Res 83:711–730

Kingwell K (2013) Neuro-oncology: everolimus for astrocytoma in tuberous sclerosis complex. Nat Rev Neurol 9:6. https://doi.org/10.1038/nrneurol.2012.257

Kutty RK et al (2001) Molecular characterization and developmental expression of NORPEG, a novel gene induced by retinoic acid. J Biol Chem 276:2831–2840

Kutty RK et al (2006) Cell density-dependent nuclear/cytoplasmic localization of NORPEG (RAI14) protein. Biochem Bioph Res Co 345:1333–1341

Lee D et al (2007) IKK beta suppression of TSC1 links inflammation and tumor angiogenesis via the mTOR pathway. Cell 130:440–455

Li S et al (2008) Genome-wide coactivation analysis of PGC-1alpha identifies BAF60a as a regulator of hepatic lipid metabolism. Cell Metab 8:105–117. https://doi.org/10.1016/j.cmet.2008.06.013

Li J, Tang Y, Cai D (2012) IKKbeta/NF-kappaB disrupts adult hypothalamic neural stem cells to mediate a neurodegenerative mechanism of dietary obesity and pre-diabetes. Nat Cell Biol 14:999–1012. https://doi.org/10.1038/ncb2562

Li J et al (2016) Nuclear PKC-theta facilitates rapid transcriptional responses in human memory CD4 + T cells through p65 and H2B phosphorylation. J Cell Sci 129:2448–2461. https://doi.org/10.1242/jcs.181248

Liu Y et al (2017) Peripheral immune tolerance alleviates the intracranial lipopolysaccharide injection-induced neuroinflammation and protects the dopaminergic neurons from neuroinflammation-related neurotoxicity. J Neuroinflamm 14:223. https://doi.org/10.1186/s12974-017-0994-3

Peng YF et al (2000) Ankycorbin: a novel actin cytoskeleton-associated protein. Genes Cells 5:1001–1008

Qian X, Mruk DD, Cheng CY (2013) Rai14 (retinoic acid induced protein 14) is involved in regulating f-actin dynamics at the ectoplasmic specialization in the rat testis*. PLoS ONE 8:e60656. https://doi.org/10.1371/journal.pone.0060656

Subhan F et al (2017) Fish scale collagen peptides protect against CoCl2/TNF-alpha-induced cytotoxicity and inflammation via inhibition of ROS, MAPK, and NF-kappaB pathways in HaCaT cells. Oxid Med Cell Longev 2017:9703609. https://doi.org/10.1155/2017/9703609

Temiz-Resitoglu M et al (2017) Activation of mTOR/IκB-α/NF-κB pathway contributes to LPS-induced hypotension and inflammation in rats. Eur J Pharmacol 802:7–19. https://doi.org/10.1016/j.ejphar.2017.02.034

Thoreen CC, Chantranupong L, Keys HR, Wang T, Gray NS, Sabatini DM (2012) A unifying model for mTORC1-mediated regulation of mRNA translation. Nature 485:109–113. https://doi.org/10.1038/nature11083

Vitiello D, Neagoe P, Sirois MG, White M (2015) Effect of everolimus on the immunomodulation of the human neutrophil inflammatory response and activation. Cell Mol Immunol 12:40–52. https://doi.org/10.1038/cmi.2014.24

Wendel H et al (2004) Survival signalling by Akt and eIF4E in oncogenesis and cancer therapy. Nature 428:332–337

Yang T, Li D, Liu F, Qi L, Yan G, Wang M (2015) Regulation on Beclin-1 expression by mTOR in CoCl2-induced HT22 cell ischemia-reperfusion injury. Brain Res 1614:60–66. https://doi.org/10.1016/j.brainres.2015.04.016

Yun S et al (2016) 4EBP1/c-MYC/PUMA and NF-kappaB/EGR1/BIM pathways underlie cytotoxicity of mTOR dual inhibitors in malignant lymphoid cells. Blood 127:2711–2722. https://doi.org/10.1182/blood-2015-02-629485